Stable Interest Point Detection under Illumination Changes Using Colour Invariants

Flore Faille
Institute for Real-Time Computer Systems
Technische Universität München, 80290 Munich
Flore.Faille@rcs.ei.tum.de

Abstract

Stable interest point detection is relevant for many computer vision applications. However, most detectors are sensitive to illumination changes, as their response varies with image contrast. In the best case, detection stability is increased using a simple image formation model assuming that illumination effects cause slowly varying changes in the image. This does not accurately model shadows and shading (interaction between illumination and scene geometry). Therefore, a new detection method is presented here, which is based on the very popular Harris detector and on the *m* space [5]. It yields a detection which is invariant to shadows, shading and illumination colour for matte surfaces. A preprocessing scheme is proposed to reduce the sensitivity to colour artifacts caused by demosaicing. The new detector is evaluated on real images acquired under different illuminations by comparison with other interest point detectors. The detection stability is well enhanced, especially for scenes with complex geometry.

1 Introduction

Interest point detection is relevant for many computer vision applications, such as e.g. registration, image retrieval, object recognition and localisation. Stable detection is a prerequisite for reliable applications: Ideally the same interest points should be detected under all imaging conditions. Many detectors were designed for grey–value images, based on various principles like local extrema [9, 17], curvature maxima along contours [15], analysis of the local grey–value distribution [16], maxima of the local autocorrelation function [7]. However, the detector responses are all sensitive to image contrast. Therefore detection is sensitive to illumination changes, which frequently occur when images taken at distant time instants are handled. One exception is the detector based on phase congruency by Kovesi [8]. Yet its prohibitively high computing time limits its usability.

To handle this sensitivity to illumination changes, most applications detect as many interest points as possible using a low detection threshold, and subsequently characterise and match their neighbourhood with illumination invariant descriptors and robust matching algorithms (see e.g. [9, 13, 17]). Increasing the stability of interest point detection under lighting changes would reduce the number of outliers and decrease matching complexity. Surprisingly, little has been done to reach this goal despite the numerous illumination invariant descriptors like [5, 9, 11, 13, 17, 18]. Therefore, in previous work [2, 4],

BMVC 2005 doi:10.5244/C.19.19

we enhanced the stability of the Harris detector [7] at a moderate complexity increase by compensating the local lighting conditions. A simple image formation model is used: photometric changes caused by illumination are modelled by local affine transformations of the grey–values (local multiplicative transformations in [4]). In [2], detectors based on local derivative normalisation, on local cornerness function normalisation and on local thresholding are compared. In [4] a fast homomorphic detector is presented. The Harris detector is chosen as basis because of its wide use and of its stability under varying camera position [15]. The homomorphic algorithm in [4] could be easily adapted to any detector based on high–pass filtering, e.g. [9, 12]. Detection stability increases, especially when complex lighting changes occur due for example to light source movements [2, 4]. Yet, the used image formation model is inaccurate near depth or surface normal discontinuities (e.g. near 3D corners), near sharp shadow patterns, near specularities and near colour edges, limiting the achievable stability [2, 4].

Only few interest point detectors exist for colour images, as texture information is almost fully contained in pixel intensity: Even if colour descriptors are used, interest point detection can be applied to intensity images, as in [17]. However, colour information could help to reduce the sensitivity to illumination, as image formation can be more accurately modelled, e.g. with the dichromatic reflection model. In [11], bicolour neighbourhoods are detected by estimating the local colour distribution. As no geometry information and a randomised grid are used for detection, the neighbourhoods have no specific location in the image, restricting their use to recognition tasks. In [13], the Harris detector is extended for colour images using the Di Zenzo colour gradient. This colour Harris detector is as sensitive to illumination changes as the original Harris detector. In [18] robust methods are introduced to compute shadow–shading invariant derivatives and shadow–shading–specular invariant derivatives. The invariant derivatives are shown to enhance the stability of the colour Harris detector on synthetic images. Yet the used assumption of white illumination reduces the applicability because there exists no reliable method to correct automatically illumination colour on real images [1].

Therefore, the colour Harris detector is enhanced in this paper using the m space [5], which yields invariants to illumination colour, shadows and shading for matte surfaces. Section 2 gives a short overview over colour invariants and explains our choice for the m space. The new detector and an implementation robust to noise and demosaicing artifacts are described in section 3. Finally, an experimental evaluation on real images and a conclusion are given in sections 4 and 5.

2 Colour Invariants

Shadows, shading, illumination colour and specularities can be modelled with the dichromatic reflection model (see e.g. [5, 11, 18]). Assuming narrow–band colour filters, the measured colour values C^R, C^G and C^B at a pixel (x,y) can be expressed as:

$$C^i = m_b(\mathbf{l},\mathbf{s})L^iS^i + m_s(\mathbf{l},\mathbf{s},\mathbf{v})L^i, \text{ for } i = R,G \text{ and } B. \quad (1)$$

The first term models body (or Lambertian) reflection. The second term models surface (or specular) reflection. m_b and m_s express the geometric dependencies of these terms as a function of the light direction $\mathbf{l}$, of the surface normal $\mathbf{s}$ and of the viewing direction $\mathbf{v}$. S^i is the i^{th} sensor response to surface reflectance under white illumination. L^i is the illumination factor for channel i.

If m_b, m_s and L^i are assumed to vary slowly in space, photometric changes caused by illumination can be modelled by local affine transformations for each colour channel independently. It generalises the model for grey–value images used in [2, 4, 9]. Illumination invariant features can be obtained e.g. by a local normalisation of the channels as in [13, 17]. However, effects due to sharp shadow patterns, specularities and shading near discontinuities of the scene geometry are not modelled accurately, as in the case of grey–value images. Only illumination colour changes are more accurately modelled.

For matte surfaces, m_s is assumed to be zero. The influence of shading (modelled by m_b) and of shadows (modelled by $L^i \rightarrow \alpha L^i$) becomes a multiplicative factor common to all channels C^i. Therefore, shadow and shading invariants can be obtained by building ratios between channels, like the normalised colour values (e.g. $r = C^R/(C^R + C^G + C^B)$) in [5, 11] or the robust invariant in [18] which is less noise sensitive. The last factor influencing Lambertian reflection is the illuminant colour (L^R, L^G, L^B). The latter can be compensated using white balancing. However, the existing automatic white balancing methods are not reliable on real images [1]. Manual white balancing is not always practicable. Furthermore, it cannot deal with scenes lighted by several light sources, for which (L^R, L^G, L^B) may change for different scene points. An alternative consists in building invariants to illumination colour, assuming that (L^R, L^G, L^B) varies slowly in space. This assumption holds for most scene points, except at the boundary between surfaces lighted by different illuminants and near sharp coloured shadows. To achieve invariance, colour ratios for two neighbouring pixels (x_1, y_1) and (x_2, y_2) are used in [5, 11]:

$$m_1 = \frac{C^R(x_1,y_1)}{C^G(x_1,y_1)} \frac{C^G(x_2,y_2)}{C^R(x_2,y_2)} = \frac{L^R S^R(x_1,y_1)}{L^G S^G(x_1,y_1)} \frac{L^G S^G(x_2,y_2)}{L^R S^R(x_2,y_2)} = \frac{S^R(x_1,y_1)}{S^G(x_1,y_1)} \frac{S^G(x_2,y_2)}{S^R(x_2,y_2)}. \quad (2)$$

m_1 only depends on the surface reflectances S^R and S^G at pixels (x_1, y_1) and (x_2, y_2). m_2 and m_3 are defined similarly for C^R/C^B and C^B/C^G ratios. m_1, m_2 and m_3 form the m space [5], which yields invariants to shadows, shading and illumination colour for matte surfaces. The components are best calculated in the logarithmic domain, as ratios are transformed to differences. The transformation from RGB space is then given by:

$$\ln m_1 = (\ln C^R(x_1,y_1) - \ln C^R(x_2,y_2)) - (\ln C^G(x_1,y_1) - \ln C^G(x_2,y_2)). \quad (3)$$

$\ln m_2$ and $\ln m_3$ are obtained similarly. By construction, the m space components are only different from zero at boundaries between areas with different colours.

Under the assumption of white illumination, hue H [5] and the robust shadow–shading–specular invariant derivatives in [18] provide illumination invariance for any type of surfaces. However, these invariants cannot be used in practice due to the unreliability of automatic white balancing methods [1].

3 Illumination Invariant Colour Interest Point Detection

3.1 Detection Algorithm

The proposed interest point detector is based on the colour Harris detector [13] and on the m space [5], which yields invariance to shadows, shading and illumination colour for matte surfaces. The principles of the colour Harris detector [13] are summarised shortly

here. The texture around pixel (x,y) is represented by the matrix $\mathbf{M}$:

$$\mathbf{M} = G(\sigma) \otimes \sum_{i=R,G,B} \begin{bmatrix} {C_x^i}^2 & C_x^i C_y^i \\ C_x^i C_y^i & {C_y^i}^2 \end{bmatrix}, \tag{4}$$

where $G(\sigma)$ is a Gaussian with standard deviation σ (in this paper $\sigma = 3.0$) and $\otimes$ is the convolution operator. C_x^i and C_y^i are the derivatives of the image channel C^i in x and y directions. They are estimated by convolution with the derivatives of a Gaussian (here with $\sigma_{deriv} = 1.2$). The interest points are the local maxima of the cornerness function CF with a cornerness value above the user–defined detection threshold T ($T > 0$):

$$CF = \mathrm{Det}(\mathbf{M}) - \alpha \, \mathrm{Tr}^2(\mathbf{M}), \text{ here with } \alpha = 0.06 \text{ [7, 13].} \tag{5}$$

According to eqs. (2) and (3), the derivatives of $\ln C^R - \ln C^G$, $\ln C^R - \ln C^B$ and $\ln C^B - \ln C^G$ enable the computation of an illumination invariant texture matrix $\mathbf{M}$ for matte surfaces (see eq. (6) for more details). This results in stable interest point detection under illumination changes for matte scenes.

Colour invariants are noise sensitive especially in dark image areas, due to the use of ratios or of the logarithmic transformation. In addition, pixels with values equal to zero cannot be handled. Like in [4], $\ln(1 + C^i)$ is used instead of $\ln C^i$: It is only a minor approximation for most pixel values and reduces noise sensitivity in dark areas. Some noise reducing preprocessing can also be applied, as discussed in section 3.2. The high correlation between colour channels can be used to reduce computing time and noise influence: Only the two least noisy components[1] of the m space $\ln C^R - \ln C^G$ and $\ln C^B - \ln C^G$ are taken into account to compute $\mathbf{M}$. In experimental evaluations, this 2–channel detector achieved similar or higher stability than the 3–channel detector, independently of the colours present in the scene. In summary, the m space Harris detector is:

1. Apply preprocessing to reduce noise (see section 3.2).
2. Perform the logarithmic transformation using $l^i = \ln(1 + C^i)$ for $i = R, G$ and B.
3. Convolve $(l^R - l^G)$ and $(l^B - l^G)$ with the derivatives of a Gaussian.
4. Compute the illumination invariant texture matrix:

$$\mathbf{M} = G(\sigma) \otimes \sum_{i=R,B} \begin{bmatrix} {(l^i - l^G)_x}^2 & (l^i - l^G)_x (l^i - l^G)_y \\ (l^i - l^G)_x (l^i - l^G)_y & {(l^i - l^G)_y}^2 \end{bmatrix}. \tag{6}$$

5. Compute the cornerness function CF according to eq. (5).
6. Detect all local maxima of CF with a cornerness value above the user–defined threshold T ($T > 0$).

A major difference to the original Harris detector is the nature and the number of detected interest points. The new detector relies on chrominance. Interest points are only detected near boundaries between areas having different colours, as shown in figure 4. This new illumination invariant detection framework can also be adapted to edge detectors or other interest point detectors based on high–pass filtering (e.g. [9, 12]).

[1] In current cameras, the green and the blue channels have typically the highest and the lowest noise.

(a) (b) (c) (d)

Figure 1: Enlarged detail of a colour image: (a) image reconstructed with ACPI demosaicing [6], (b) image reconstructed with WACPI demosaicing [10], (c) ACPI image after colour Nagao filter, (d) WACPI image after colour Nagao filter.

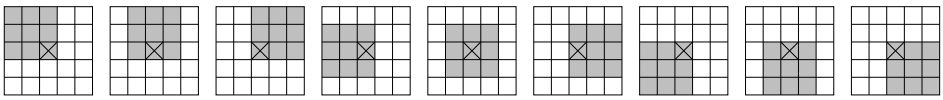

Figure 2: The nine windows used for the (simplified) colour Nagao filter are shown in grey. The currently processed pixel is marked with a cross.

3.2 Image Acquisition and Preprocessing

Some preprocessing is required to decrease noise sensitivity in dark areas caused by the logarithmic transformation (step 1 in section 3.1). The preprocessing used in [4] to handle this problem for grey–value images can be extended to colour images: For each channel, values $C^i(x,y)$ $(i = R,G,B)$ smaller than the experimentally chosen threshold c are replaced by the mean value in their 3×3 neighbourhood. The threshold c must be adapted to the sensor noise. For our experimental setting, $c = 3$ performs well.

The use of colour images brings an additionnal noise source: Most digital colour cameras have a single CCD or CMOS sensor and measure only one colour (e.g. R, G or B) per pixel by means of a colour filter array (CFA). Therefore, an interpolation of the colour information, named demosaicing, is necessary to obtain a three channel image. Demosaicing introduces artifacts, such as wrong colours, which appear especially near edges as shown in figure 1 (a). The image was reconstructed with the Adaptive Colour Plane Interpolation (ACPI) [6], a fast state–of–the art demosaicing algorithm. Colour invariants are sensitive to wrong colour artifacts. The artifacts decrease detection stability as they vary with the imaging conditions. Several state–of–the–art and recently developed demosaicing methods are compared in [3] to find the method best suited for computer vision tasks. The Weighted Adaptive Colour Plane Interpolation (WACPI) [10] achieves the highest reconstruction quality near colour edges [3], so it is applied here. As shown in figure 1 (b), WACPI demosaicing yields better reconstruction quality.

Unlike marginal preprocessing (where colour channels are filtered independently from each other as in the method above), vector preprocessing (where pixels are considered as (C^R, C^G, C^B) vectors) can reduce wrong colour artifacts and noise. The Nagao filter [14] achieves a good correction of colour artifacts. In comparison to [14], the shape of the nine windows is simplified for faster processing (see figure 2). The total variance $\sigma^2 = \sigma_R^2 + \sigma_G^2 + \sigma_B^2$ is estimated for all windows. The (C^R, C^G, C^B) value of the processed pixel is set to the mean value (μ_R, μ_G, μ_B) of the smallest variance window. The results are shown in figures 1 (c) and (d). As the mean of the nine most similar pixels is built,

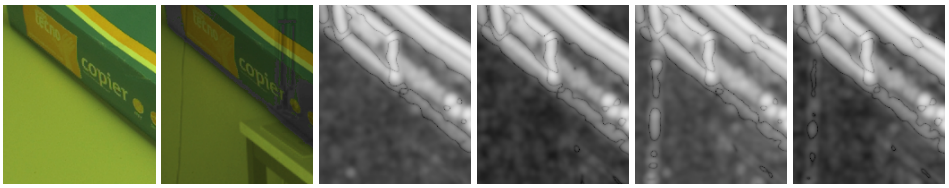

(a) (b) (c) (d) (e) (f)

Figure 3: Influence of a simulated intensity change and demosaicing artifacts on the cornerness function CF of the m space Harris detector (For visualisation, $\ln|CF|$ is displayed scaled between 0 and 255): (a) original image, (b) image after intensity change, (c) $\ln|CF|$ for marginal preprocessing, (d) $\ln|CF|$ for Nagao filter, (e) $\ln|CF|$ for marginal preprocessing and demosaicing artifacts, (f) $\ln|CF|$ for Nagao filter and demosaicing artifacts.

colour artifacts, which are most of the time isolated colour outliers, almost disappear and edges are sharpened. On the other hand, high frequency details which are difficult to interpolate correctly are filtered out, resulting in inaccurate texture.

The influence of demosaicing artifacts on the m space Harris detector is illustrated in figure 3. An intensity change is simulated on an image by: $C^i(x,y) \mapsto f(x,y)C^i(x,y)$ for $i = R,G$ and B, where $f(x,y)$ is a single channel image with values between 0 and 1. Such a transformation could be caused by shadows or shading (see eq. (1)). The original and the modified images are shown in figures 3 (a) and (b). If the cornerness function is computed on the modified three channel image, the intensity change can be compensated as in theory (see eq. (2)): No significant filter response occurs near the introduced pure intensity edges for both preprocessing types (see figures 3 (c) and (d)). However, if the modified image is sampled with a CFA and demosaiced before detection, the detector response is influenced by the intensity edges when marginal preprocessing is applied (see figure 3 (e)). This is caused by the inevitable demosaicing inaccuracies. This influence is reduced if the colour Nagao filter is applied as preprocessing (see figure 3 (f)). Alternatively, demosaicing quality can be improved if possible. The main drawback of the Nagao preprocessing is a loss of texture information. Therefore, the experimental evaluation of section 4 will be performed for both preprocessing types.

4 Experimental Evaluation

The m space Harris detector (MSHD) with both preprocessing types (MSHD+marginal and MSHD+Nagao) is evaluated by comparing it to the colour Harris detector (CHD) [13], to the homomorphic Harris detector for grey–value images (HHD+GV) [4] and to the Harris detector based on robust shadow–shading invariants (RIHD)[2] [18]. For this, images are acquired with the Basler A302fc single–chip colour CCD camera and with WACPI demosaicing [10]. For several scenes, image series are obtained by varying the type (natural light, neon lamps or tungsten halogen lamps), number, position and direction of the light source(s). For the m space detector (MSHD+marginal and MSHD+Nagao), the detection threshold T is set to 10^{-5}. To improve the CHD stability under lighting changes, the N interest points with the highest cornerness values are detected ($N = 200$).

[2]The author would like to thank J. van de Weijer for his help for the implementation of the RIHD method

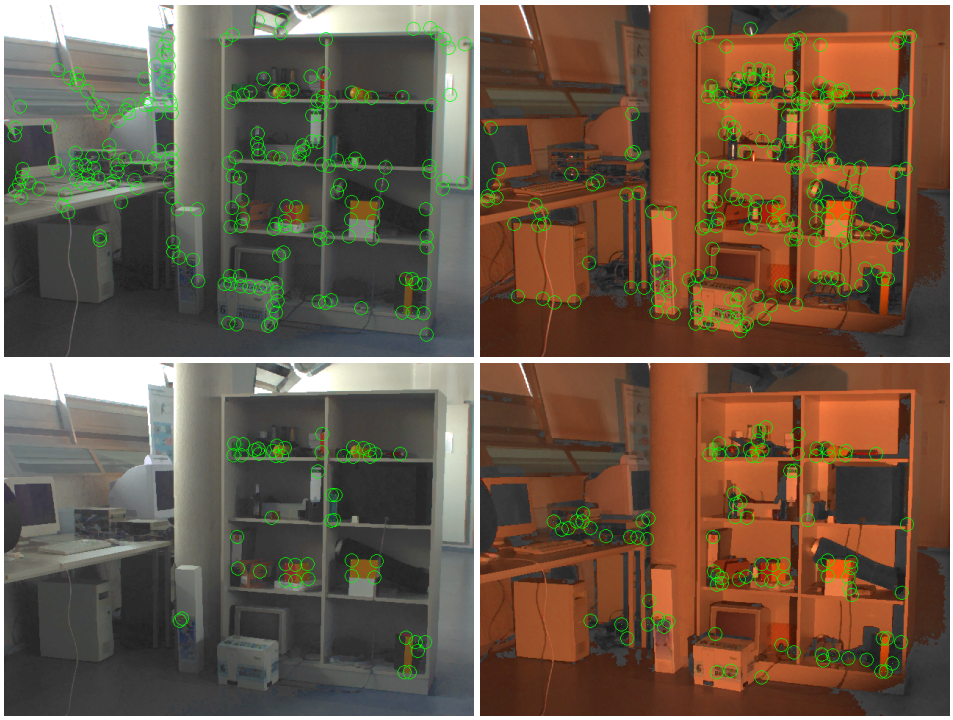

Figure 4: Detection example on images showing a scene under two different illuminants (left: sunlight, right: tungsten halogen lamp). Circles indicate interest points. Top: colour Harris detector [13]. Bottom: m space Harris detector with Nagao preprocessing.

The HHD+GV allows to evaluate stability increase due to the use of colour images, as it achieves a stability enhancement similar to the algorithms in [2] with a lower computing time. T is set to 10^{-4} for HHD+GV. To obtain grey–value images, the luminance component of the YUV colour space is computed: $Y = 0.3C^R + 0.59C^G + 0.11C^B$. For the RIHD, T is set to $2.5 \cdot 10^{-7}$ and the white patch algorithm is applied to correct illumination colour, as it yields good results on real images [1].

To estimate stability, one image is chosen as reference in the series. The interest points detected in the other images are compared to the interest points of the reference image (the reference interest points). An interest point is considered redetected if it is in the 3×3 neighbourhood of a reference interest point. For each image, the detection stability can be characterised e.g. by the repeatability rate [15]. The use of the following two rates is preferred here as it is more descriptive: Redetection and false positive rates. The redetection rate is the number of redetected points divided by the number of reference points. Repeatability and redetection rates are equal when the same number of interest points is detected in all images. However, this is not the case when a detection threshold is applied. The false positive rate is the number of detected points without correspondance to any reference interest point divided by the number of detected points. Saturated areas reduce detection stability, as image information gets lost. To compensate this effect, which does not depend on the detector but on the image data, interest points near saturated areas

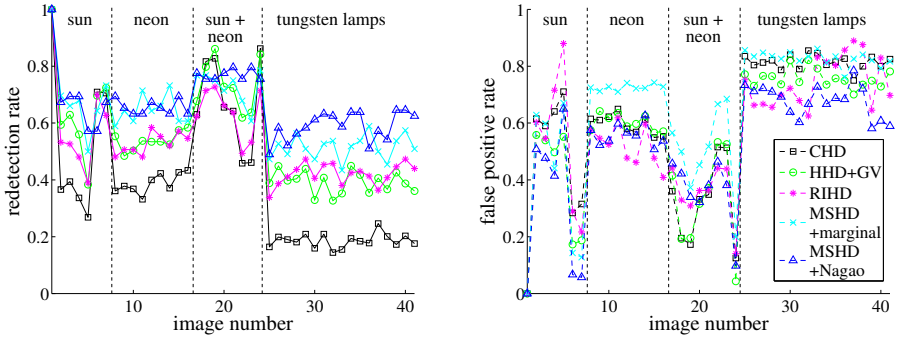

Figure 5: Detection stability for a complex scene with varying type, number, position and orientation of the light sources. Redetection and false positive rates are indicated with straight and dashed lines, respectively. Images 1 and 25 are shown in figure 4.

in either image are not taken into account for rate estimation.

A detection example on two images used in the evaluation is shown in figure 4 for the MSHD+Nagao and for the CHD. With the m space Harris detector, interests points are detected near edges between areas of different colours. Therefore, less interest points are obtained. Stability is however increased as shown in figure 5, because shading and shadow influences are reduced. So, the m space Harris detector is suitable for applications requiring few but stable interest points, such as hypothesis generation for registration, object recognition or localisation. As threshold T is low, the noise sensitivity of the m space Harris detector, which cannot be entirely suppressed by preprocessing, is visible in figure 4: False positives appear in dark areas and in high frequency areas (where demosaicing accuracy is low). They disappear for higher T. Therefore, noise level depends on image content. Image acquisition should achieve a compromise between the size of saturated areas and the size of dark areas. As far as complexity is concerned, the MSHD+marginal and the MSHD+Nagao require approximately 8% and 61% more computing time than the CHD. For comparison, the RIHD needs 101% more computing time than the CHD. The HHD+GV is the fastest method: It requires 32% less computing time than the CHD.

The detection stability for a scene with complex 3D geometry is presented in figure 5. The CHD achieves by far the worst stability, as it only compensates lighting changes causing the same variation for all channels and all pixels. The MSHD+Nagao yields the best stability. In comparison, the MSHD+marginal achieves similar redetection rates but it is more sensitive to noise (the false positive rate is higher). The RIHD yields slightly better stability than the HHD+GV. For all detectors, worse results occur for tungsten lamps as they produce a less diffuse illumination and darker, hence noisier, green values.

The results for two scenes with simple 3D geometry are given in figure 6. As above, the CHD is the least stable detector. The stability discrepancy between the m space Harris detector and the HHD+GV decreases, as shading has less influence on image data. The performance of the MSHD+marginal is also improved, as the images contain less high frequency areas, hence less demosaicing artifacts. For the series on the left, two illuminant types are used simultaneously. As a consequence, white balancing does not work accurately, especially for images 4, 9 and 12 (see figure 6). This reduces the stability of

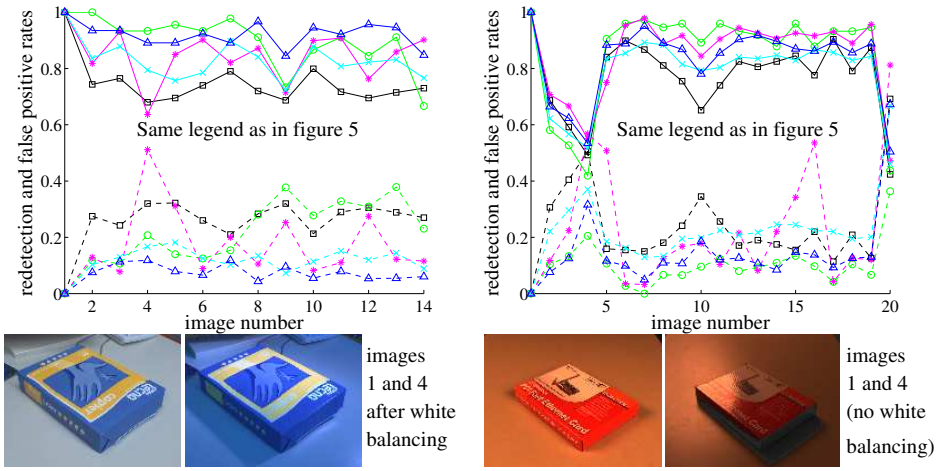

Figure 6: Detection stability for two simple scenes under varying number, position and orientation of the light sources (right: neon and tungsten lamps, left: tungsten lamps).

the RIHD which relies on white balancing. The HHD+GV and the CHD cannot compensate illuminant colour changes, hence the *m* space Harris detector (MSHD+marginal and MSHD+Nagao) achieves the best stability. The series on the right shows a specular object and allows to evaluate the sensitivity of the *m* space Harris detector to specularities. Here, the HHD+GV and the RIHD perform best. The RIHD is more sensitive to noise in dark image areas than the *m* space Harris detector, as shown by the numerous false positives for images 4, 16 and 20.

5 Conclusion

A new interest point detector for colour images, the *m* space Harris detector, is proposed to enhance detection stability under illumination changes. It is based on the Harris detector and on the *m* space, which yields invariants to shadows, shading and illumination colour for matte surfaces. As the algorithm relies on chrominance information, interest points are detected only near edges between areas of different colours. The *m* space Harris detector delivers fewer but more stable interest points than the usual detectors. However, the algorithm is sensitive to wrong colour artifacts occuring in images acquired with single–chip colour cameras. Therefore, high quality demosaicing methods should be preferred in applications, for example WACPI [10]. The images can also be preprocessed with the colour Nagao filter to reduce colour artifacts. The *m* space Harris detector was evaluated on real images showing scenes under varying illumination. For this, it was compared to the colour Harris detector [13], to the homomorphic Harris detector for grey–value images [4] and to the Harris detector based on robust shadow–shading invariants [18]. The *m* space Harris detector yields the highest stability, especially when the scene geometry is complex. A drawback is its sensitivity to specularities. To improve the results, automatic methods could be used to adapt the detection threshold to the demosaicing noise level, which depends on image data. Future work also includes a compensation or at least a

detection of specularities. Finally, the stability under simultaneous illumination change and camera movement will be analysed.

References

[1] K. Barnard, L. Martin, A. Coath, and B. Funt. A comparison of computational color constancy algorithms – part II: Experiments with image data. *IEEE Trans. on Image Processing*, 11(9):985–996, September 2002.

[2] F. Faille. Adapting interest point detection to illumination conditions. In *Digital Image Computing: Techniques and Applications (DICTA)*, pages 499–508, 2003.

[3] F. Faille. Comparison of demosaicking methods for color information extraction. In *Proc. of the International Conference on Computer Vision and Graphics (ICCVG)*, 2004.

[4] F. Faille. A fast method to improve the stability of interest point detection under illumination changes. In *Proc. of the International Conference on Image Processing (ICIP)*, 2004.

[5] T. Gevers and A. W. M. Smeulders. Color–based object recognition. *Pattern Recognition*, 32(3):453–464, March 1999.

[6] J. Hamilton and J. Adams. Adaptive color plane interpolation in single sensor color electronic camera. US Patent 5,629,734, 1997.

[7] C. Harris and M. Stephens. A combined corner and edge detector. In *Proc. of the 4th Alvey Vision Conference*, 1988.

[8] P. Kovesi. Phase congruency detects corners and edges. In *Digital Image Computing: Techniques and Applications (DICTA)*, pages 309–318, 2003.

[9] D. G. Lowe. Distinctive image features from scale–invariant keypoints. *International Journal of Computer Vision*, 60(2):91–110, November 2004.

[10] W. Lu and Y. P. Tan. Color filter array demosaicking: New method and performance measures. *IEEE Trans. on Image Processing*, 12(10):1194–1210, October 2003.

[11] J. Matas, D. Koubaroulis, and J. Kittler. Colour image retrieval and object recognition using the multimodal neighbourhood signature. In *Proc. of the European Conference on Computer Vision (ECCV)*, pages 48–64, June 2000.

[12] K. Mikolajczyk and C. Schmid. An affine invariant interest point detector. In *Proc. of the European Conference on Computer Vision (ECCV)*, pages 128–142, 2002.

[13] P. Montesinos, V. Gouet, R. Deriche, and D. Pelé. Matching color uncalibrated images using differential invariants. *Image and Vision Computing*, 18(9):659–672, June 2000.

[14] M. Nagao and T. Matsuyama. Edge preserving smoothing. *Computer Graphics and Image Processing*, 9(4):394–407, April 1979.

[15] C. Schmid, R. Mohr, and C. Bauckhage. Evaluation of interest point detectors. *International Journal of Computer Vision*, 37(2):151–172, June 2000.

[16] S. M. Smith and J. M. Brady. SUSAN – a new approach to low level image processing. *International Journal of Computer Vision*, 23(1):45–78, May 1997.

[17] T. Tuytelaars. *Local, Invariant Features for Registration and Recognition*. PhD thesis, Katholieke Universiteit Leuven, 2000.

[18] J. van de Weijer. *Color Features and Local Structure in Images*. PhD thesis, University of Amsterdam, March 2005.